

SCIENTIFIC REPORTS



OPEN

Navigation in bile acid chemical space: discovery of novel FXR and GPBAR1 ligands

Received: 01 April 2016
Accepted: 16 June 2016
Published: 06 July 2016

Claudia Finamore¹, Carmen Festa¹, Barbara Renga², Valentina Sepe¹, Adriana Carino², Dario Masullo¹, Michele Biagioli², Silvia Marchianò², Angela Capolupo³, Maria Chiara Monti³, Stefano Fiorucci² & Angela Zampella¹

Bile acids are signaling molecules interacting with nuclear receptors and membrane G-protein-coupled receptors. Among these receptors, the farnesoid X receptor (FXR) and the membrane G-coupled receptor (GPBAR1) have gained increasing consideration as druggable receptors and their exogenous dual regulation represents an attractive strategy in the treatment of enterohepatic and metabolic disorders. However, the therapeutic use of dual modulators could be associated to severe side effects and therefore the discovery of selective GPBAR1 and FXR agonists is an essential step in the medicinal chemistry optimization of bile acid scaffold. In this study, a new series of 6-ethylcholane derivatives modified on the tetracyclic core and on the side chain has been designed and synthesized and their *in vitro* activities on FXR and GPBAR1 were assayed. This speculation resulted in the identification of compound 7 as a potent and selective GPBAR1 agonist and of several derivatives showing potent dual agonistic activity.

Next to their ancestral roles in lipid digestion and solubilization, bile acids (BAs), the principal constituent of bile, are today recognized signaling molecules involved in many physiological functions and these signaling pathways involve the activation of several metabolic nuclear receptors, mainly the BAs sensor FXR^{1,2}, and the dedicated membrane G-protein-coupled receptor, GPBAR1 (TGR5)³.

Principally, FXR functions as a sensor of bile acid level playing an important role in the regulation of their intracellular levels in hepatocytes⁴. FXR is activated by CDCA (1)^{1,2,5} and upon CDCA binding, FXR forms a heterodimer with the retinoid X receptor (RXR) that binds specific DNA sequences within the promoter regions of target genes. The canonical gene expression program activated by FXR leads to the reduction in the intracellular bile acid levels by increasing the export of bile acids out of cells, decreasing bile acid uptake and decreasing bile acid synthesis^{6–8}. As a consequence, FXR has been identified as an appealing target in the treatment of cholestasis disorders such as primary biliary cirrhosis (PBC) and liver steatosis^{9–11}, two severe human conditions in which bile acids homeostasis is impaired.

PBC is an immunologically mediated progressive liver disease characterized by the destruction of small intrahepatic bile ducts, with accumulation of bile acids in the liver and consequently inflammation, fibrosis, and potential cirrhosis. Fatigue and pruritus are the most common symptoms of primary biliary cirrhosis, and both can be debilitating in some patients. Cholestasis causes intense, sometimes intolerable, itch leading to scratching, excoriation, sleep deprivation, and depression¹².

In addition, FXR plays a crucial beneficial role in hepatic triglyceride homeostasis, as well as in glucose metabolism and therefore, FXR agonists are also promising for the treatment of non-alcoholic fatty liver disease (NAFLD), dyslipidemia and type 2 diabetes (T2DM)^{13–16}.

In addition to FXR and other nuclear hormone receptors, BAs can also signal through a membrane-receptor (GPBAR1/TGR5/M-BAR)³. The most potent endogenous GPBAR1 activator is TLCA (2) followed by DCA, while other BAs are less potent. GPBAR1^{-/-} mice display prolonged cholestasis, exacerbated inflammatory response and more severe liver injury after partial hepatectomy¹⁷. In addition, in a mouse model of xenobiotic (DDC)-induced sclerosing cholangitis, mice overexpressing GPBAR1 showed less liver injury while mice lacking

¹Department of Pharmacy, University of Naples "Federico II", Via D. Montesano, 49, 80131 Naples, Italy. ²Department of Surgery and Biomedical Sciences, Nuova Facoltà di Medicina, P.zza L. Severi 1, 06132 Perugia, Italy. ³Department of Pharmacy, University of Salerno, Via Giovanni Paolo II, 132, 84084 Fisciano (Salerno), Italy. Correspondence and requests for materials should be addressed to A.Z. (email: angela.zampella@unina.it)

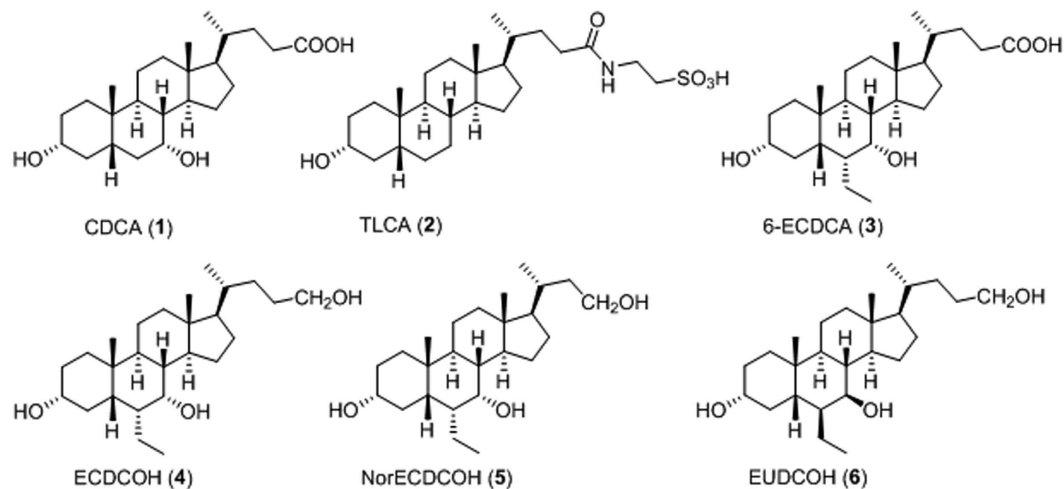


Figure 1. CDCA and TLCA, the most potent endogenous activators of FXR and GPBAR1, respectively. 6-ECDCA and 6 α -ethylchenodeoxycholanol derivatives 4 and 5 as dual ligands and EUDCOH (6), a selective GPBAR1 agonist.

GPBAR1 showed aggravation of inflammation and fibrosis¹⁸. Collectively, these findings suggest a critical role of GPBAR1 for liver protection against BA overload but activation of GPBAR1 should be also associated with severe side effects, especially in the context of impaired bile acid level in the liver.

In fact, GPBAR1 has been recently identified as the physiological mediator of pruritus¹⁹, a common symptom observed in cholestasis and the severity of this side effect limits the pharmacological utility of dual agonists in the treatment of primary biliary cirrhosis (PBC) and related cholestatic disorders.

On the other hand, responses to GPBAR1 activation include increased energy expenditure, improved intestinal motility, glucose metabolism and insulin sensitivity^{20,21}. The latter two occur through the release of the glucagon-like peptide 1 (GLP-1) by intestinal L cells upon GPBAR1 activation²². Therefore, the exogenous regulation of this receptor represents an attractive strategy to treat metabolic disorders such as NASH, hypercholesterolemia, hypertriglyceridemia, and T2DM^{23,24}. Thus, in the window of metabolic disorders, the development of ligands endowed with dual activity toward GPBAR1 and FXR appears to be a promising strategy^{23–26}. In contrast, the discovery of highly selective FXR agonists could represent a new frontier in the treatment of primary biliary cirrhosis (PBC) and related cholestatic disorders where the concomitant activation of GPBAR1 could increase patient risk for adverse side effects. Indeed, results from PBC phase II clinical trial with 6-ECDCA/OCA (3), a potent semi-synthetic steroidal FXR agonist²⁷, have shown that while the compound exerts benefit, its use has associated with pruritus. In fact, up to 40% of PBC patients halted the treatment due to the severity of itching in one trial and approx. 80% of patients experienced the symptoms. The reason why OCA causes itching is unclear. However, this agent is almost equally potent on FXR and GPBAR1^{28,29} and it is predictable that the severity of this side effect could prevent its use in stage III and IV PBC patients³⁰.

Medicinal chemistry on 6-ECDCA scaffold and on bile acid scaffold has produced several derivatives modified on the side chain in the length and in the nature of the end-group and on the tetracyclic core^{11,31–33}. Indeed these derivatives cover the same chemical space of BAs that are intrinsically promiscuous toward FXR and GPBAR1 and therefore, with few exceptions, this kind of speculation mainly afforded dual modulators³³. The most interesting results have been obtained with compounds 4–6 (Fig. 1).

The replacement of the negative charged end group with a neutral polar group produced derivative 4, again a potent dual agonist and the above activity was also maintained by the corresponding *nor*-derivative 5, with one carbon less on the side chain. Of interest compound 5 attenuates liver damage in animal models of non-obstructive cholestasis without inducing itching³⁴. Finally, speculation on stereochemical modification on ring B produced 6, a C-24 alcohol that represents the first example of ursodeoxycholanol derivative substituted at C-6 with a β -oriented ethyl group. Pharmacological assays demonstrated that this derivative is a rather potent ligand for GPBAR1 (EC_{50} 1.03 μ M) failing in transactivating FXR at any concentration tested²⁶.

Recently we have also demonstrated that compound 6 exerts portal pressure-lowering effects in rodent models of portal hypertension by directly regulating the expression/activity of cystathionine γ -lyase (CSE) and endothelial nitric oxide synthases (eNOS) in liver sinusoidal endothelial cells (LSEC), thus affirming this compound as a novel approach to attenuate the hemodynamic changes in patients with liver cirrhosis³⁵.

In addition, in our recent contribution, we have extended the structure-activity relationship on C24 6-ethylcholane scaffold modifying the hydroxyl group at C-3 and demonstrating that the elimination or the inversion of the above functionality on ring A could shift the activity toward FXR³⁶.

Prompted by these promising results, we decided to expand our investigation proceeding in the modification of the side chain length on the 6-ethylcholane scaffold. As shown in the Fig. 2, a small library of C23 6-substituted cholane derivatives, compounds 7–15, have been prepared.

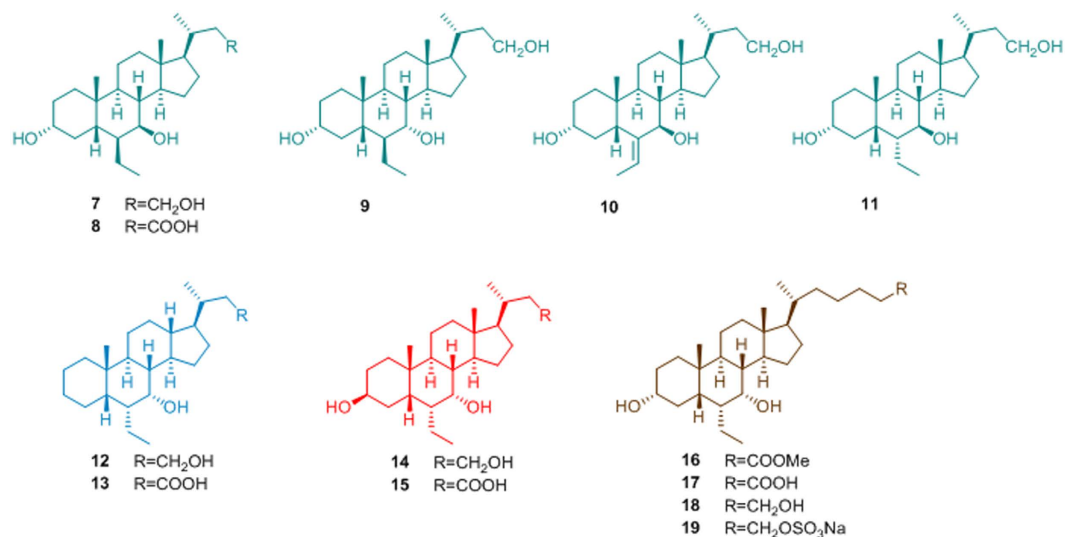


Figure 2. 6-Ethylcholane derivatives generated in this study.

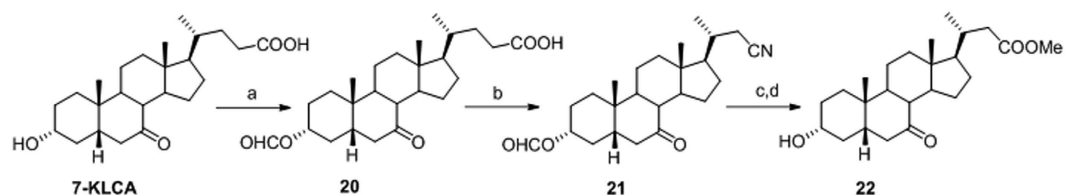


Figure 3. Preparation of 7-keto-norLCA methyl ester (**22**). Reagents and conditions: (a) HCOOH, HClO₄; (b) TFA, trifluoroacetic anhydride, NaNO₂; (c) KOH 30% in MeOH/H₂O 1:1 v/v, 66% over three steps; (d) p-TsOH, MeOH dry, quantitative yield.

In this framework, the effects of the stereochemical arrangement of the cholane C-6/C-7 positions and the substituents adorning the C-3 position and the C-23 side chain end group (OH or COOH) have been explored in term of potency/selectivity toward FXR and GPBAR1.

In addition, the chemical diversity of available bile acid receptor modulators have been increased preparing bis-*homo* 6-ethylcholane derivatives **16–19**. Pharmacological investigations resulted in the identification of compounds **7** and **19** as a potent and selective GPBAR1 agonist and a potent dual agonist respectively.

Results

In the synthesis of 6-ethyl *nor*cholane derivatives **7–15**, the first step was the preparation of the key intermediate 7-keto-*nor*LCA methyl ester **22** from 7-KLCA (Fig. 3). A reaction sequence comprising Fisher's esterification with formic acid and perchloric acid generated the formiate derivative **20** that was subjected to a Beckmann rearrangement with treatment with sodium nitrite in a trifluoroacetic anhydride/trifluoroacetic acid mixture obtaining the 23-nitrile derivative **21**³⁷. Prolonged alkaline hydrolysis afforded the corresponding carboxylic acid that was in turn transformed in the methyl ester derivative **22** by methanol/*p*-toluensulfonic acid treatment (66% yield from 7-KLCA).

Preparation of 3 α -hydroxy-6-ethyl*nor*cholane derivatives. Acetylation at C-3 on **22** and aldolic addition to a silyl enol ether intermediate generated the intermediate **23** (60% over three steps) that was hydrogenated at the exocyclic double bond (H₂ on Pd(OH)₂) affording exclusively the 6 β -ethyl group in the compound **24** (quantitative yield). Treatment of **24** with an excess of NaBH₄ in methanol followed by LiBH₄ reduction on the crude reaction product to secure the reduction at the methyl ester on the side chain, gave the concomitant deacetylation at C-3 and reduction at C-7 keto and at C-23 methyl ester groups (Fig. 4).

HPLC purification gave the main product **7** and small amount of its epimer at C-7, compound **9**. When intermediate **24** was treated with a stoichiometric amount of NaBH₄, the reduction occurred exclusively at C-7 keto group giving the methyl ester **25**, that was subjected to basic hydrolysis furnishing the carboxylic acid **8** in 82% over two steps.

Intermediate **23** was also used as starting material in the preparation of **10** and **11**. Sodium borohydride/LiBH₄ treatment on **23** proceeded in a stereoselective manner, affording the exclusive formation of 7 β -hydroxyl derivative as judged by the shape of H-7 as a doublet ($J = 9.8$ Hz) which is consistent with an axial disposition for this proton, and therefore with the β -orientation of the hydroxyl group on ring B. Dipolar couplings H-7/H-24

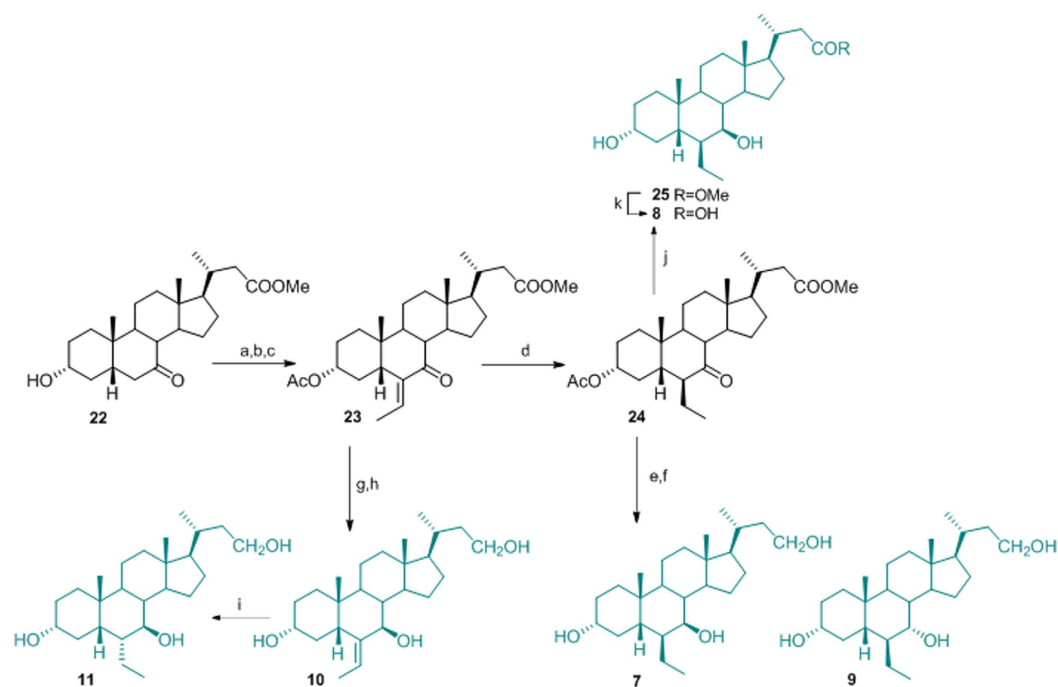


Figure 4. Synthesis of 3 α -hydroxy-6-ethylnorcholane derivatives. Reagents and conditions: (a) acetic anhydride, pyridine; (b) DIPA, *n*-BuLi, TMSCl, TEA dry, THF dry -78°C ; (c) acetaldehyde, $\text{BF}_3(\text{OEt})_2$, CH_2Cl_2 , -60°C , 60% over three steps; (d) H_2 , $\text{Pd}(\text{OH})_2$, THF/MeOH 1:1, quantitative yield; (e) NaBH_4 , MeOH dry, 0°C ; (f) LiBH_4 , MeOH, THF dry, 0°C , 77% over two steps; (g) NaBH_4 , MeOH; (h) LiBH_4 , MeOH dry, THF, 0°C , 85% over two steps; (i) H_2 , $\text{Pd}(\text{OH})_2$, THF:MeOH 1:1 v/v, quantitative yield; (j) NaBH_4 , MeOH dry, 0°C ; (k) NaOH, MeOH:H₂O 1:1 v/v, 82% over two steps.

and Me-25/H-5 in the NOESY spectrum allowed definition the E configuration for the exocyclic double bond as depicted in **10**. Hydrogenation on $\text{Pd}(\text{OH})_2$ catalyst afforded derivative **11** with the ethyl group at C-6 α -oriented.

Preparation of 3-deoxy- and 3 β -hydroxy-6 α -ethylnorcholane derivatives. In the preparation of 3-deoxy- and 3 β -hydroxy-6-ethylnorcholane derivatives **12–15**, a convergent protocol was applied starting from the methyl ester **24**, that was first treated with MeONa in methanol to effect de-acetylation at C-3 and inversion at C-6 and then with tosyl chloride to afford **26** in 73% yield over two steps (Fig. 5).

Elimination by $\text{LiBr}/\text{Li}_2\text{CO}_3$ treatment and hydrogenation of the unsaturated-ring A transient intermediate furnished **27** that was used as starting material for the preparation of compounds **12** and **13**.

LiBH_4 treatment produced the concomitant reduction at C-24 methyl ester and at C-7 carbonyl group furnishing **12** whereas alkaline hydrolysis of the methyl ester followed by LiBH_4 treatment gave **10** in high chemical yield.

Finally, treatment of the tosyl derivative **26** with potassium acetate in DMF/H₂O afforded inversion at C-3 on **28**. Reduction at C-7 and C-24 with LiBH_4 and hydrolysis at methyl ester group on the side chain gave **14** and **15**, respectively.

Preparation of bis-homo 6-ethylcholane derivatives. In the preparation of bis-homo-6-ethylcholane derivatives **16**, a four-steps reaction sequence on **29**, previously prepared in our laboratory^{25,26}, including protection of the alcoholic functions at C3 and C7, reduction of the side chain methyl ester, and subsequent one pot Swern oxidation/Wittig C2 homologation, gave the protected methyl ester of $\Delta^{24,25}$ bis-homoECDCA **31** (Fig. 6).

Side chain double bond hydrogenation and alcoholic function deprotection gave the methyl ester **16** that was used as starting material in the preparation of the carboxylic acid **17** and the corresponding alcohol **18** through treatment with LiOH and LiBH_4 , respectively. Chemoselective sulfation at C-26 hydroxyl group on a small aliquot of **18** gave the corresponding sulfate derivative **19**³⁸.

Discussion and Conclusion

Derivatives **7–19** were tested in the luciferase reporter assays on HepG2 and HEK-293T cells transfected with FXR and GPBAR1, respectively. Data shown in Fig. 7, panel A, reporting the results of the transactivation assay on FXR, reaffirm the 6 α /7 α stereochemical arrangement around ring B as the most important feature in FXR activity with derivatives **7–11**, with one or two substituents on ring B in β configuration, devoid of any activity at 10 μM dose. Of interest is the behavior of derivatives **12–15**, with both substituents on ring B in α -configuration and a shortened (C23) side chain. In a cross comparison between the above compounds, it is quite evident that the presence of a negative charge on the side chain favors the 3-deoxy derivatives (compare **13** with COOH vs **12** with CH_2OH), whereas the alcoholic function at C-24 improves FXR activity of the corresponding 3 β -hydroxyl

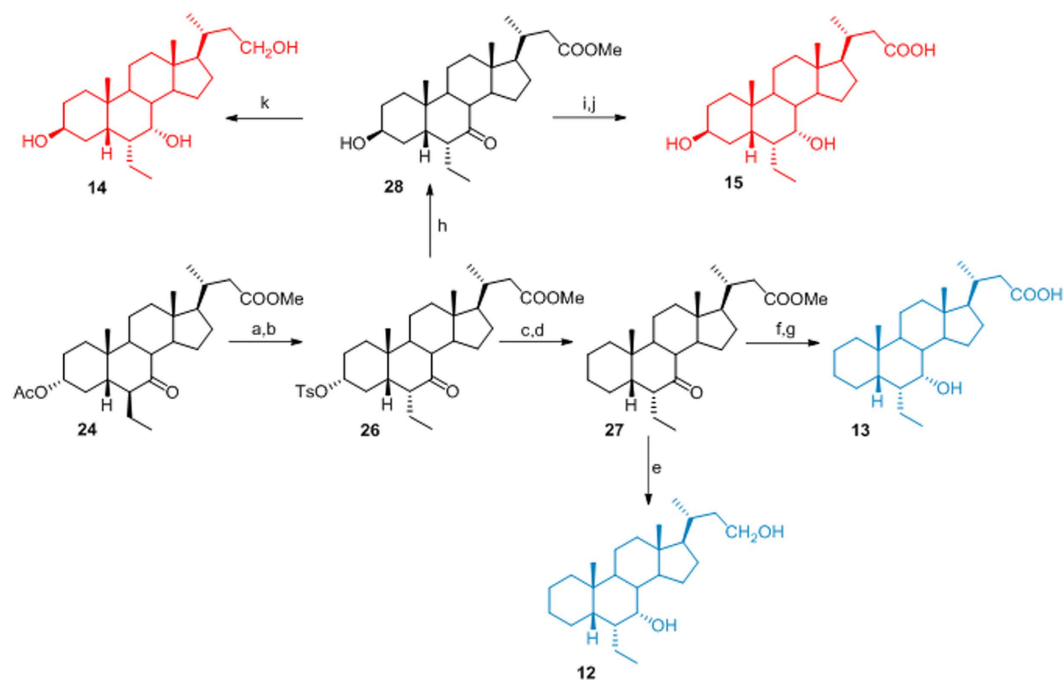


Figure 5. Synthesis of 3-deoxy- and 3 β -hydroxy-6 α -ethylnorcholane derivatives. *Reagents and conditions:* (a) MeONa, MeOH; (b) p-TsCl, pyridine, 73% over two steps; (c) LiBr, Li₂CO₃, DMF, reflux, (d) H₂, Pd(OH)₂, THF/MeOH 1:1, room temperature, quantitative yield over two steps; (e) LiBH₄, MeOH dry, THF, 0 °C, 70%; (f) NaOH, MeOH:H₂O 1:1 v/v; (g) LiBH₄, MeOH dry, THF, 0 °C, 92% over two steps; (h) CH₃COOK, DMF:H₂O 5:1 v/v; (i) NaOH, MeOH:H₂O 1:1 v/v; (j) LiBH₄, MeOH dry, THF, 0 °C, 58% over two steps; (k) LiBH₄, MeOH dry, THF, 0 °C, 57%.

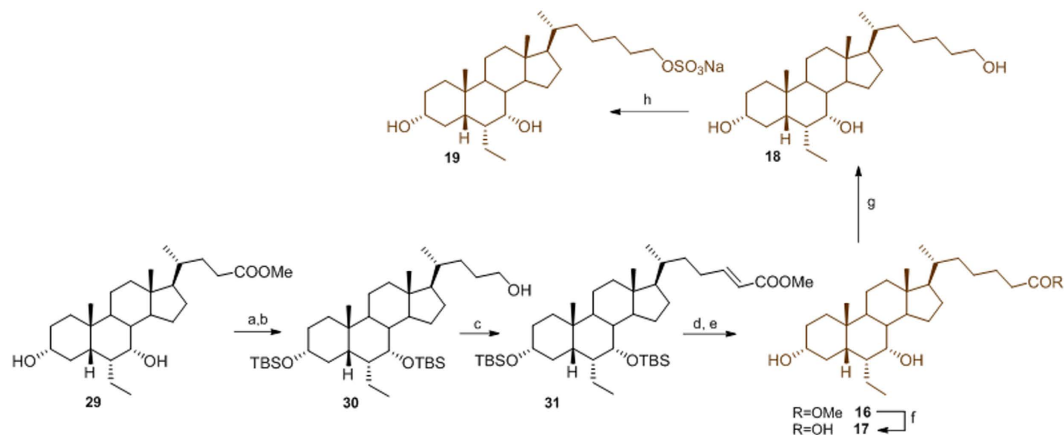


Figure 6. Preparation of bis-homo 6-ethylcholane derivatives. *Reagents and conditions:* (a) 2,6-lutidine, t-butyltrimethylsilyl trifluoromethanesulfonate, CH₂Cl₂, 0 °C; (b) LiBH₄, MeOH dry, THF, 0 °C, 68% over two steps; (c) DMSO, oxalyl chloride, TEA dry, CH₂Cl₂, -78 °C then methyl(triphenylphosphoranylidene)acetate, 79%; (d) H₂, Pd(OH)₂/C Degussa type, THF/MeOH 1:1, quantitative yield; (e) HCl 37%, MeOH, 88%; (f) NaOH 5% in MeOH/H₂O 1:1 v/v, 89%; (g) LiBH₄, MeOH dry, THF, 0 °C, 78%; (h) Et₃N·SO₃, DMF, 95 °C, 25%.

derivative (compare **14** with CH₂OH vs **15** with COOH). In addition, results on derivatives **16–19** demonstrate that side chain elongation on the 6-ethyl scaffold could be instrumental in generation potent FXR agonists. In this subset, the nature of the side chain end group produces a remarkable effect in FXR transactivation with the sulfate derivative **19**, the most potent FXR agonist generated in this study.

Results of transactivations of CREB-responsive elements in HEK-293T transiently transfected with the membrane bile acid receptor GPBAR1 are showed in Fig. 7, panel B. Compounds **7** and **8**, with both the ethyl and the hydroxyl groups on ring B β -oriented, were demonstrated inducers of cAMP-luciferase reporter gene, with **7** showing a potency similar to that of TLCA (**2**), the most potent endogenous GPBAR1 agonist. As expected, all derivatives with both substituents on ring B in α -configuration are endowed with GPBAR1 agonistic activity, and

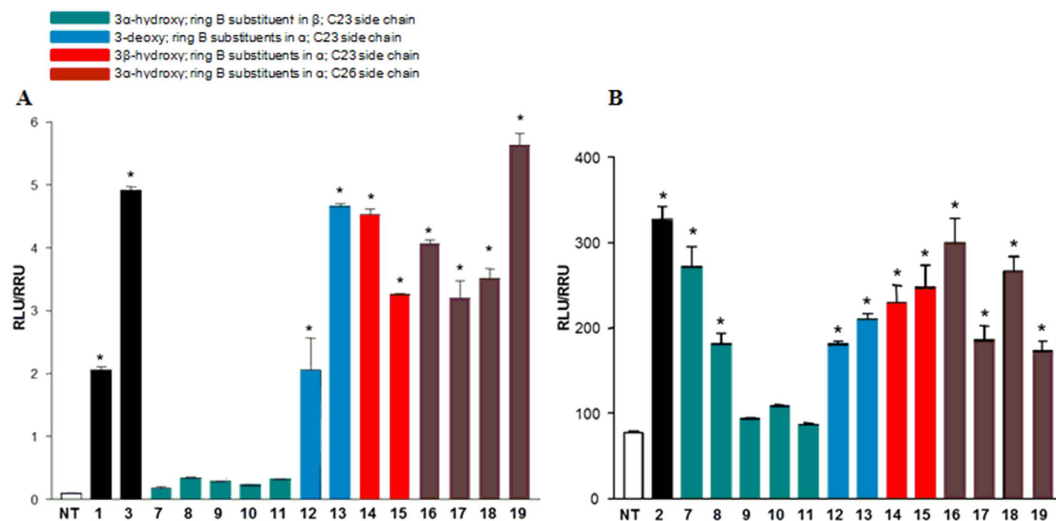


Figure 7. Agonism on bile acid receptors by transactivation assay. (A) HepG2 cells were transfected with pSG5-FXR, pSG5-RXR, pCMV- β gal, and p(hsp27)TKLUC vectors. Cells were stimulated with compounds 7–19 (10 μ M). CDCA (1, 10 μ M) and 6-ECDCA (3, 1 μ M) were used as a positive control. (B) HEK-293T cells were co-transfected with GPBAR1 and a reporter gene containing a cAMP responsive element in front of the luciferase gene. Cells were stimulated with 7–19 (10 μ M). TLCA (2, 10 μ M) was used as a positive control. Luciferase activity served as a measure of the rise in intracellular cAMP following activation of GPBAR1. In both panels, results are expressed as mean \pm standard error. * $p < 0.05$ versus not treated cells (NT).

the above activity is quite independent of the length and the functionalization of the side chain and by the substitution at C-3 with 3 α -, 3 β -hydroxy and 3-deoxy derivatives sharing a similar behavior. Even if, by comparing FXR and GPBAR1 transactivation results, derivatives 12–19 are to be considered dual agonists, there is a considerable difference in GPBAR1 activity of C26 derivatives 16–19. It is quite evident that the presence of a neutral (COOMe in 16) or a non-charged polar group (CH₂OH in 18) on the elongated side chain is preferable respect to a negative charged end group such as the COOH in 17 and the sulfate in 19.

The relative potency of selected members of this novel family was then investigated by a detailed measurement of the concentration-response curve of the 3-deoxy C-23 carboxylic acid derivative 13, the 3 β -hydroxyl C-23 alcohol 14 and the C-26 sulfate derivative 19, all sharing the 6 α /7 α configuration, on FXR and GPBAR1 transactivation.

As illustrated in Figs 8 and 9, compounds 13, 14, and 19 transactivate FXR with an EC₅₀ of 2.3 μ M, 5.3 μ M and 1.7 μ M, respectively. In addition, 13, 14, and 19 transactivate GPBAR1 with EC₅₀ of 4.3 μ M, 1.0 μ M and 0.95 μ M, respectively. Combining these data, compound 19 represents the most potent FXR/GPBAR1 dual agonist identified in this study. Finally, compound 7 exerted a concentration-dependent effect on activation of cAMP responsive element in HEK-293T cells transfected with GPBAR1 with an EC₅₀ of 0.91 μ M.

The ability of compound 19, the most potent FXR agonist in these series, in the recruitment of the coactivator SRC-1 was also measured through Alpha screen technology. CDCA (1) and 6-ECDCA (3) were used as positive controls at 2 μ M concentration and the effect of 6-ECDCA (3) was settled as 100%. As shown in Fig. 10, panel A, compound 19 showed an activity in the recruitment of SRC-1 co-activator at least comparable, if not better, to that measured for 3, thus confirming the transactivation results. Interestingly, the presence of the non-conjugable functional group such as the sulfate group on the side chain instead of the carboxyl end group as in 6-ECDCA (3) points the attention on the positive pharmacokinetic properties of compound 19 and therefore on its therapeutic potential in liver FXR mediated diseases. On the other hand, panel A in Fig. 10 shows compounds 7, 9 and 10 completely unable to recruit SRC-1 in cell free Alpha screen assay, thus excluding any pharmacokinetic elements in their FXR inactivity on cellular luciferase assays (Fig. 7, panel A) and indirectly reaffirming compound 7 as a selective GPBAR1 agonist (Fig. 7, panel B).

RT-PCR further confirmed 19 as a dual FXR/GPBAR1 agonist and the GPBAR1 mediated pharmacological effect of compound 7. As shown in Fig. 10 panels B–D, 19 was able to induce the expression of BSEP and OST α , two canonical FXR targeted genes, whereas both compounds increased pro-glucagon gene expression in GLUTag cells. The observed 2 fold of BSEP upregulation as well as the robust induction of OST α mRNA is consistent with the activation of the FXR-mediated effect by compound 19³⁹.

In summary, a series of 6-ethylcholane derivatives were designed and synthesized and all the newly synthesized compounds were evaluated *in vitro* for their activity towards FXR and GPBAR1. Concerning the structural features, α -substituents introduced at C-6 and C-7 positions play a significant role in FXR and GPBAR1 activity, with all derivatives showing this configurational disposition able to transactivate both receptors. Even if the sulfate derivative 19 is the most potent FXR agonist discovered in this study, the dual modulation is a general trend within compounds 12–19, independently by the length and the functional group of the side chain as well as by the substitution at C-3. On the contrary, modification at the configurational disposition of one or both substituents

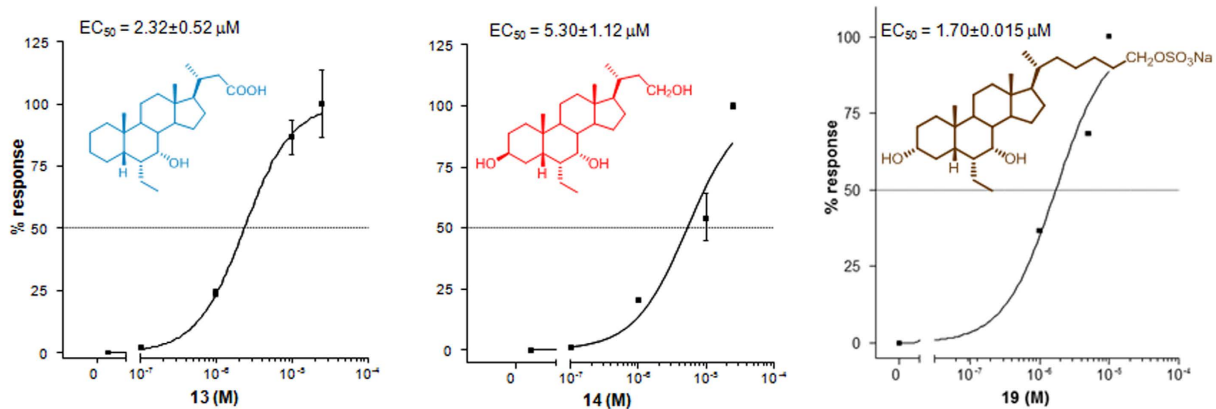


Figure 8. Concentration-response curve of 13, 14, and 19 on FXR. HepG2 cells were transfected with FXR as described above and used in a luciferase reporter assay. Twenty-four hour post transfection cells were stimulated with increasing concentrations of each agent: range from 100 nM to 25 μ M. Results are expressed as mean \pm standard error.

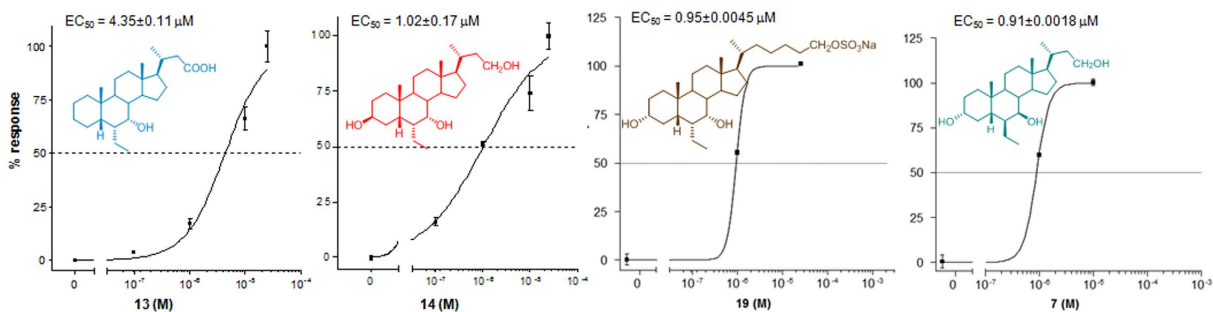


Figure 9. Concentration-response curve of compounds 13, 14 and 19 on FXR. HepG2 cells were transfected with FXR as described above and used in a luciferase reporter assay. Twenty-four hour post transfection cells were stimulated with increasing concentrations of each agent: range from 100 nM to 25 μ M. Results are expressed as mean \pm standard error.

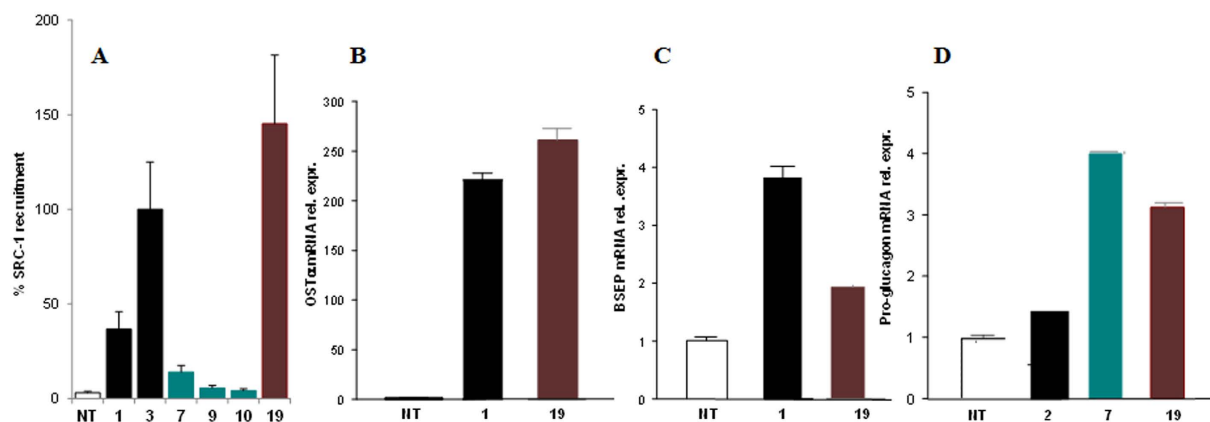


Figure 10. (A) Coactivator recruitment assay measuring a direct interaction of FXR with SRC-1; ligands at 2 μ M. Results are expressed as percentage of the effect of 3 arbitrarily settled as 100%. NT is referred to the experiment in absence of ligand. Results are expressed as mean \pm standard error. (B,C) Real-time PCR analysis of mRNA expression on FXR target genes BSEP (B), and OST α (C) in HepG2 cells primed with 10 μ M of compound 19. CDCA (1) was used as a positive control at 10 μ M. (D) Real-time PCR analysis of mRNA expression of GPBAR1 target gene Pro-glucagon in GLUTAg cells stimulated with 10 μ M of compounds 7 and 19, and TLCA (2) used as a positive control at 10 μ M. Values are normalized to GAPDH and are expressed relative to those of not treated cells (NT) which are arbitrarily settled to 1. The relative mRNA expression is expressed as $2(-\Delta\Delta Ct)$.

on ring B is clearly deleterious in term of FXR activation but represents a promising strategy in the identification and development of selective GPBAR1 agonists with compound 7, the most potent GPBAR1 activator identified in this study.

Methods

Chemistry. Specific rotations were measured on a Jasco P-2000 polarimeter. High-resolution ESI-MS spectra were performed with a Micromass Q-TOF mass spectrometer. NMR spectra were obtained on Varian Inova 400, 500 and 700 NMR spectrometers (^1H at 400 and 700 MHz, ^{13}C at 100 and 175 MHz, respectively) equipped with a SUN microsystem ultra5 hardware and recorded in CD_3OD ($\delta_{\text{H}} = 3.30$ and $\delta_{\text{C}} = 49.0$ ppm) and CDCl_3 ($\delta_{\text{H}} = 7.26$ and $\delta_{\text{C}} = 77.0$ ppm). All of the detected signals were in accordance with the proposed structures. Coupling constants (J values) are given in Hertz (Hz), and chemical shifts (δ) are reported in ppm and referred to CHD_2OD and CHCl_3 as internal standards. Spin multiplicities are given as s (singlet), br s (broad singlet), d (doublet), or m (multiplet). Through-space ^1H connectivities were evidenced using NOESY experiment with mixing time of 400 ms. HPLC was performed with a Waters Model 510 pump equipped with Waters Rheodine injector and a differential refractometer, model 401. Reaction progress was monitored via thin-layer chromatography (TLC) on Alugram silica gel G/UV254 plates. Silica gel MN Kieselgel 60 (70–230 mesh) from Macherey-Nagel Company was used for column chromatography. All chemicals were obtained from Sigma-Aldrich, Inc. Solvents and reagents were used as supplied from commercial sources with the following exceptions. Tetrahydrofuran and triethylamine were distilled from calcium hydride immediately prior to use. Methanol was dried from magnesium methoxide as follow. Magnesium turnings (5 g) and iodine (0.5 g) are refluxed in a small (50–100 mL) quantity of methanol until all of the magnesium has reacted. The mixture is diluted (up to 1 L) with reagent grade methanol, refluxed for 2–3 h then distilled under nitrogen. All reactions were carried out under argon atmosphere using flame-dried glassware. The purities of compounds were determined to be greater than 95% by HPLC.

Synthetic procedures. See the Supporting Information.

Transactivation assay. For FXR and GPBAR1 mediated transactivations, HepG2 cells and HEK293T cells were transfected as described previously²⁵. At 24 h post-transfection, cells were stimulated 18 h with $10\ \mu\text{M}$ CDCA (1), TLCA (2), 6-ECDCA (3) and compounds 7–19. After treatments, $20\ \mu\text{L}$ of cellular lysates were read using Dual Luciferase Reporter Assay System (Promega Italia s.r.l., Milan, Italy) according manufacturer specifications using the Glomax 20/20 luminometer (Promega Italia s.r.l., Milan, Italy). To evaluate GPBAR1 mediated transactivation, HEK-293T cells were transfected with 200 ng of human pGL4.29 (Promega), a reporter vector containing a cAMP response element (CRE) that drives the transcription of the luciferase reporter gene luc2P, with 100 ng of pCMVSPORT6-human GPBAR1, and with 100 ng of pGL4.70. Dose-response curves were performed in HepG2 and HEK-293T cells transfected as described above and then treated with increasing concentrations of compounds 7 (1 – $10\ \mu\text{M}$), 13, 14 and 19 ($100\ \text{nM}$ – $25\ \mu\text{M}$). At 18 h post stimulations, cellular lysates were assayed for luciferase and Renilla activities using the Dual-Luciferase Reporter assay system (E1980, Promega). Luminescence was measured using Glomax 20/20 luminometer (Promega). Luciferase activities were normalized with Renilla activities.

RNA isolation and RT-PCR. Total RNA was isolated from HepG2 or GLUTAg cells using the TRIzol reagent according to the manufacturer's specifications (Invitrogen). One microgram of purified RNA was treated with DNase-I and reverse transcribed with Superscript II (Invitrogen). For Real Time PCR, 10 ng template was dissolved in $25\ \mu\text{L}$ containing 200 nmol/L of each primer and $12.5\ \mu\text{L}$ of $2 \times$ SYBR FAST Universal ready mix (Invitrogen). All reactions were performed in triplicate, and the thermal cycling conditions were as follows: 2 min at $95\ ^\circ\text{C}$, followed by 40 cycles of $95\ ^\circ\text{C}$ for 20 s and $60\ ^\circ\text{C}$ for 30 s in iCycler iQ instrument (Biorad). The relative mRNA expression was calculated and expressed as $2^{-\Delta\Delta\text{Ct}}$. Forward and reverse primer sequences were the following: human GAPDH, gaagtggaaggtcggagt and catgggtggaatcatattggaa; human OST α , tgttgggccctttccaatac and ggctcccatgttctgctcac; human BSEP, gggccattgtacgagatcctaa and tgcaccgtctttcacttctctg; mouse GAPDH, ctgag-tatgtcgtggagtctac and gttggtggtgcaggatgcattg; mouse Pro-glucagon, tgaagacaacgcctcactac and caatgtttccgggtcttc.

Direct interaction on FXR by Alpha screen technology in a coactivator recruitment assay.

Anti-GST-coated acceptor beads were used to capture the GST-fusion FXR-LBD whereas the biotinylated-SRC-1 peptide was captured by the streptavidin donor beads. Upon illumination at 680 nm, chemical energy is transferred from donor to acceptor beads across the complex streptavidin-Donor/Src-1-Biotin/GSTFXR-LBD/Anti-GST-Acceptor and a signal is produced. The assay was performed in white, low-volume, 384-well Optiplates (PerkinElmer) using a final volume of $25\ \mu\text{L}$ containing final concentrations of 10 nM of purified GST-tagged FXR-LBD protein, 30 nM biotinylated Src-1 peptide, $20\ \mu\text{g}/\text{mL}$ anti-GST acceptor beads acceptor beads and $10\ \mu\text{g}/\text{mL}$ of streptavidin donor bead (PerkinElmer). The assay buffer contained 50 mM Tris (pH 7.4), 50 mM KCl, 0.1% BSA, and 1 mM DTT. The stimulation times with $1\ \mu\text{L}$ of tested compound (dissolved in 50% DMSO/ H_2O) were fixed to 30 min at room temperature. The concentration of DMSO in each well was maintained at a final concentration of 4%. After the addition of the detection mix (acceptor and donor beads) the plates were incubated in the dark for 4 h at room temperature and then were read in Envision microplate analyzer (PerkinElmer).

References

- Makishima, M. *et al.* Identification of a nuclear receptor for bile acids. *Science* **284**, 1362–1365 (1999).
- Parks, D. J. *et al.* Bile acids: natural ligands for an orphan nuclear receptor. *Science* **284**, 1365–1368 (1999).
- Maruyama, T. *et al.* Identification of membrane type receptor for bile acids (M-BAR). *Biochem. Biophys. Res. Commun.* **298**, 714–719 (2002).

4. Modica, S., Gadaleta, R. M. & Moschetta, A. Deciphering the nuclear bile acid receptor FXR paradigm. *Nucl. Recept. Signal.* **8**, e005 (2010).
5. Wang, H., Chen, J., Hollister, K., Sowers, L. C. & Forman, B. M. Endogenous bile acids are ligands for the nuclear receptor FXR/BAR. *Mol. Cell.* **3**, 543–553 (1999).
6. Goodwin, B. *et al.* A regulatory cascade of the nuclear receptors FXR, SHP-1, and LXR-1 represses bile acid biosynthesis. *Mol. Cell.* **6**, 517–526 (2000).
7. Ananthanarayanan, M., Balasubramanian, N., Makishima, M., Mangelsdorf, D. J. & Suchy, F. J. Human bile salt export pump promoter is transactivated by the farnesoid X receptor/bile acid receptor. *J. Biol. Chem.* **276**, 28857–28865 (2001).
8. Boyer, J. L. *et al.* Upregulation of a basolateral FXR-dependent bile acid efflux transporter OSTalpha-OSTbeta in cholestasis in humans and rodents. *Am. J. Physiol. Gastrointest. Liver Physiol.* **290**, G1124–G1130 (2006).
9. Fiorucci, S. & Baldelli, F. Farnesoid X receptor agonists in biliary tract disease. *Curr. Opin. Gastroenterol.* **25**, 252–259 (2009).
10. Fiorucci, S. *et al.* Targeting FXR in cholestasis: hype or hope. *Expert Opin. Ther. Targets* **12**, 1449–1459 (2014).
11. Fiorucci, S., Mencarelli, A., Distrutti, E. & Zampella, A. Farnesoid X receptor: from medicinal chemistry to clinical applications. *Future Med. Chem.* **4**, 877–891 (2012).
12. Beuers, U., Kremer, A. E., Bolier, R. & Elferink, R. P. Pruritus in cholestasis: facts and fiction. *Hepatology* **60**, 399–407 (2014).
13. Cipriani, S., Mencarelli, A., Palladino, G. & Fiorucci, S. FXR activation reverses insulin resistance and lipid abnormalities and protects against liver steatosis in Zucker (fa/fa) obese rats. *J. Lipid Res.* **51**, 771–784 (2010).
14. Rizzo, G. *et al.* The farnesoid X receptor promotes adipocyte differentiation and regulates adipose cell function *in vivo*. *Mol. Pharmacol.* **70**, 1164–1173 (2006).
15. Fiorucci, S., Rizzo, G., Donini, A., Distrutti, E. & Santucci, L. Targeting farnesoid X receptor for liver and metabolic disorders. *Trends Mol. Med.* **13**, 298–309 (2007).
16. Mencarelli, A. *et al.* Dissociation of intestinal and hepatic activities of FXR and LXR α supports metabolic effects of terminal ileum interposition in rodents. *Diabetes* **62**, 3384–3393 (2013).
17. Pean, N. *et al.* The receptor TGR5 protects the liver from bile acid overload during liver regeneration in mice. *Hepatology* **58**, 1451–1460 (2013).
18. Baghdasaryan, A. *et al.* Protective role of membrane bile acid receptor TGR5 (GPBAR1) in DDC-induced sclerosing cholangitis in mice. *J. Hepatol.* **60**, S197–S198 (2014).
19. Alemi, F. *et al.* The TGR5 receptor mediates bile acid-induced itch and analgesia. *J. Clin. Invest.* **123**, 1513–1530 (2013).
20. Watanabe, M. *et al.* Bile acids induce energy expenditure by promoting intracellular thyroid hormone activation. *Nature* **439**, 484–489 (2006).
21. Thomas, C. *et al.* TGR5-mediated bile acid sensing controls glucose homeostasis. *Cell Metab.* **10**, 167–177 (2009).
22. Parker, H.E. *et al.* Molecular mechanisms underlying bile acid-stimulated glucagon-like peptide-1 secretion. *Br. J. Pharmacol.* **165**, 414–423 (2012).
23. Fiorucci, S., Mencarelli, A., Palladino, G. & Cipriani, S. Bile-acid-activated receptors: targeting TGR5 and farnesoid-X-receptor in lipid and glucose disorders. *Trends Pharmacol. Sci.* **30**, 570–580 (2009).
24. Fiorucci, S., Cipriani, S., Baldelli, F. & Mencarelli, A. Bile acid-activated receptors in the treatment of dyslipidemia and related disorders. *Prog. Lipid Res.* **49**, 171–185 (2010).
25. D'Amore, C. *et al.* Design, synthesis, and biological evaluation of potent dual agonists of nuclear and membrane bile acid receptors. *J. Med. Chem.* **57**, 937–954 (2014).
26. Festa, C. *et al.* Exploitation of cholane scaffold for the discovery of potent and selective farnesoid X receptor (FXR) and G-protein coupled bile acid receptor 1 (GP-BAR1) ligands. *J. Med. Chem.* **57**, 8477–8495 (2014).
27. Pellicciari, R. *et al.* 6- α -Ethylchenodeoxycholic acid (6-ECDCA), a potent and selective FXR agonist endowed with anticholestatic activity. *J. Med. Chem.* **45**, 3569–3572 (2002).
28. Rizzo, G. *et al.* Functional characterization of the semisynthetic bile acid derivative INT-767, a dual farnesoid X receptor and TGR5 agonist. *Mol. Pharmacol.* **78**, 617–630 (2010).
29. Pellicciari, R. *et al.* Non genomic actions of bile acids. Synthesis and preliminary characterization of 23- and 6,23-alkyl-substituted bile acid derivatives as selective modulators for the G-protein coupled receptor TGR5. *J. Med. Chem.* **50**, 4265–4268 (2007).
30. Hirschfield, G. M. *et al.* Efficacy of obeticholic acid in patients with primary biliary cirrhosis and inadequate response to ursodeoxycholic acid. *Gastroenterology* **148**, 751–761 (2015).
31. Fiorucci, S., Zampella, A. & Distrutti, E. Development of FXR, PXR and CAR agonists and antagonists for treatment of liver disorders. *Curr. Top. Med. Chem.* **12**, 605–624 (2012).
32. Sepe, V., Distrutti, E., Limongelli, V., Fiorucci, S. & Zampella, A. Steroidal scaffolds as FXR and GPBAR1 ligands: from chemistry to therapeutic application. *Future Med. Chem.* **7**, 1109–1135 (2015).
33. Di Leva, F. S. *et al.* Structure-based drug design targeting the cell membrane receptor GPBAR1: exploiting the bile acid scaffold towards selective agonism. *Sci Rep.* **5**, 16605 (2015).
34. Cipriani, S. *et al.* Impaired itching perception in murine models of cholestasis is supported by dysregulation of GPBAR1 signaling. *PLoS One* **10**, e0129866 (2015).
35. Renga, B. *et al.* Reversal of endothelial dysfunction by GPBAR1 agonism in portal hypertension involves a AKT/FOXO1 dependent regulation of H₂S generation and endothelin-1. *PLoS One* **10**, e0141082 (2015).
36. Sepe, V. *et al.* Insights on FXR selective modulation. Speculation on bile acid chemical space in the discovery of potent and selective agonists. *Sci. Rep.* **6**, 19008 (2016).
37. Scheingart, C. D. & Hofmann, A. F. Synthesis of 24-nor-5 beta-cholan-23-oic acid derivatives: a convenient and efficient one-carbon degradation of the side chain of natural bile acids. *J. Lipid Res.* **10**, 1387–1395 (1988).
38. Goto, J., Sano, Y., Chikai, T. & Nambara, T. Synthesis of disulfates of unconjugated and conjugated bile acids. *Chem. Pharm. Bull.* **35**, 4562–4567 (1987).
39. Song, X. *et al.* Mechanistic insights into isoform-dependent and species-specific regulation of bile salt export pump by farnesoid X receptor. *J. Lipid Res.* **54**, 3030–3044 (2013).

Acknowledgements

This work was supported by grants from PSC Partners (5237 South Kenton Way, Englewood, Colorado 80111 USA) and grants from POR Campania FESR 2007-2013-O.O.2.1 (FarmaBioNet).

Author Contributions

C.F., Ca.F., V.S., D.M. and A.Z. designed and performed synthesis; B.R., A.C., S.M., M.B. and S.F. designed and performed pharmacological experiments; M.C.M. and A.C. designed and performed Alpha screen experiments; S.F. and A.Z. analyzed and interpreted the data. All authors contributed to manuscript writing and approved the final version.

Additional Information

Supplementary information accompanies this paper at <http://www.nature.com/srep>

Competing financial interests: The authors declare no competing financial interests.

How to cite this article: Finamore, C. *et al.* Navigation in bile acid chemical space: discovery of novel FXR and GPBAR1 ligands. *Sci. Rep.* **6**, 29320; doi: 10.1038/srep29320 (2016).



This work is licensed under a Creative Commons Attribution 4.0 International License. The images or other third party material in this article are included in the article's Creative Commons license, unless indicated otherwise in the credit line; if the material is not included under the Creative Commons license, users will need to obtain permission from the license holder to reproduce the material. To view a copy of this license, visit <http://creativecommons.org/licenses/by/4.0/>